JOURNAL OF SOLID STATE CHEMISTRY **61**, 197–202 (1986)

Transport Properties of Phases Belonging to the PbF_2–TaF_5 System

ALI RHANDOUR, JEAN-MAURICE REAU,
AND PAUL HAGENMULLER

*Laboratoire de Chimie du Solide du CNRS, Université de Bordeaux I,
351, cours de la Libération—33405 Talence cedex, France*

Received February 25, 1985

The transport properties of the disordered fluorite-type solid solution $Pb_{1-x}Ta_xF_{2+3x}$ ($0 \leq x \leq 0.14$) and of the ordered Pb_3TaF_{11} phase ($x = 0.25$) have been determined. For $x = 0.14$ the conductivity is shown to decrease when with diminishing disorder as a consequence of annealing. The disordered $Pb_{0.86}Ta_{0.14}F_{2.42}$ phase is an exceptionally good anionic conductor. © 1986 Academic Press, Inc.

Introduction

Several criteria leading to a high mobility of F^- ions in fluorides have been pointed out in this laboratory in the course of exhaustive studies (*1–3*): vacancies in the anionic sublattice, low coordination number of the mobile species, high polarizability of the cations, significant size difference between the involved cations, low entropy of melting, etc. These requirements have made it possible to isolate fast ionic conductors within many β-PbF_2 related systems: PbF_2–$M^{2+}F_2$ (M = Sn) (*4*), PbF_2–$M^{3+}F_3$ (M = In, Sb, Bi) (*5, 6*), PbF_2–$M^{4+}F_4$ (M = Zr, Th, U) (*7, 8*). Large domains of solid solutions whose structure derives from the fluorite type appear when Pb^{2+} in β-PbF_2 is replaced by a trivalent cation whose size is close to that of Pb^{2+} (e.g., Bi^{3+}).

These domains are reduced about by half when the substituting cation of similar size is tetravalent (e.g., Th^{4+}). As a consequence the upper limits of the solid solutions $Pb_{1-x}Bi_xF_{2+x}$ and $Pb_{1-x}Th_xF_{2+2x}$ contain approximately the same number of extra F^- anions in the fluorite-type matrix (Table I). The extent of the solid solution domains decreases when Pb^{2+} is replaced by trivalent or tetravalent cations of smaller size such as In^{3+} or Zr^{4+} (Table I).

Similar conclusions are drawn by investigating the electrical properties of the solid solutions. A maximum conductivity associated with a minimum of activation energy is observed for compositions close to $Pb_{0.75}M^{3+}_{0.25}F_{2.25}$ and $Pb_{0.875}M^{4+}_{0.125}F_{2.25}$ (Table I). A neutron diffraction study of the solid solutions $Pb_{1-x}Bi_xF_{2+x}$ and $Pb_{1-x}Th_xF_{2+2x}$ has shown that the compositions $Pb_{0.75}Bi_{0.25}F_{2.25}$ and $Pb_{0.875}Th_{0.125}F_{2.25}$ which present the best electrical performances have a large number of vacancies V_{F_1} in the normal positions of the CaF_2-type structure and are characterized by maximum disorder (*9, 10*).

The solid solutions so far investigated involved either trivalent or tetravalent substituting cations. We have studied in this work the effects of partial replacement in β-PbF_2 of the Pb^{2+} cations by a pentavalent one.

0022-4596/86 $3.00

TABLE I

Solid solution	Upper limit composition	Compositions with the best performances and $\sigma_{300\,\mathrm{K}}$
$Pb_{1-x}In_xF_{2+x}$ $(0 \le x \le 0.25)$	$Pb_{0.75}In_{0.25}F_{2.25}$	$Pb_{0.88}In_{0.12}F_{2.12}$ $\sigma_{300\,\mathrm{K}} \sim 2.10^{-4}\ \Omega^{-1}\ \mathrm{cm}^{-1}$
$Pb_{1-x}Sb_xF_{2+x}$ $(0 \le x \le 0.40)$	$Pb_{0.60}Sb_{0.40}F_{2.40}$	$Pb_{0.75}Sb_{0.25}F_{2.25}$ $\sigma_{300\,\mathrm{K}} \sim 5.10^{-4}\ \Omega^{-1}\ \mathrm{cm}^{-1}$
$Pb_{1-x}Bi_xF_{2+x}$ $(0 \le x \le 0.50)$	$Pb_{0.50}Bi_{0.50}F_{2.50}$	$Pb_{0.75}Bi_{0.25}F_{2.25}$ $\sigma_{300\,\mathrm{K}} \sim 7.10^{-5}\ \Omega^{-1}\ \mathrm{cm}^{-1}$
$Pb_{1-x}Zr_xF_{2+2x}$ $(0 \le x \le 0.18)$	$Pb_{0.82}Zr_{0.18}F_{2.36}$	$Pb_{0.90}Zr_{0.10}F_{2.20}$ $\sigma_{300\,\mathrm{K}} \sim 10^{-4}\ \Omega^{-1}\ \mathrm{cm}^{-1}$
$Pb_{1-x}Th_xF_{2+2x}$ $(0 \le x \le 0.25)$	$Pb_{0.75}Th_{0.25}F_{2.50}$	$Pb_{0.875}Th_{0.125}F_{2.25}$ $\sigma_{300\,\mathrm{K}} \sim 4.10^{-4}\ \Omega^{-1}\ \mathrm{cm}^{-1}$
$Pb_{1-x}U_xF_{2+2x}$ $(0 \le x \le 0.25)$	$Pb_{0.75}U_{0.25}F_{2.50}$	$Pb_{0.875}U_{0.125}F_{2.25}$ $\sigma_{300\,\mathrm{K}} \sim 4.10^{-4}\ \Omega^{-1}\ \mathrm{cm}^{-1}$

This substitution, which corresponds to addition of three extra F^- anions, should bring about greater increase of the number of V_{F_1} vacancies with substitution rate and, thereby improving the electrical performance. As a consequence, we studied the influence of replacing Pb^{2+} by Ta^{5+} on the electrical properties of β-PbF_2.

Experimental and Radiocrystallographic Study

The starting materials were α-PbF_2 and TaF_5 of 99.9% purity. Various mixtures of starting fluorides were well homogenized in an ultra-dry glovebox and introduced into gold tubes which were then sealed in a dry argon atmosphere. The mixtures were heated first at 100°C (a temperature slightly higher than the melting point of TaF_5) for 24 hr, and then progressively to the reaction temperature. The reactions are complete after heating at 500°C for 15 hr.

A radiocrystallographic analysis of the phases of the PbF_2–TaF_5 system obtained by quenching from 500°C has shown the existence of

For $0 \le x \le 0.14$, a disordered cubic solid solution of composition $Pb_{1-x}Ta_xF_{2+3x}$, whose structure is apparently fluorite type.

For $x = 0.25$, a definite phase with formula Pb_3TaF_{11}.

The existence range of $Pb_{1-x}Ta_xF_{2+3x}$ is less extended than those of $Pb_{1-x}Zr_xF_{2+2x}$ $(0 \le x \le 0.18)$ (*7*), $Pb_{1-x}In_xF_{2+x}$ $(0 \le x \le 0.25)$ (*5*), and $Pb_{1-x}Bi_xF_{2+2x}$ $(0 \le x \le 0.50)$ (*1*). As a consequence, the extension of the nonstoichiometry domain in the anion-excess solid solutions of fluorite type seems closely related to the size difference between the relevant cations: $r_{Ta^{5+}} = 0.88$ Å, $r_{Zr^{4+}} = 0.98$ Å, $r_{In^{3+}} = 1.06$ Å, $r_{Bi^{3+}} = 1.31$ Å, $r_{Pb^{2+}} = 1.43$ Å (ionic radii of cations in VIII coordination according to Shannon (*11*)).

The unit-cell parameter of the disordered $Pb_{1-x}Ta_xF_{2+3x}$ solid solution increases very smoothly with x from $a_F = 5.940 \pm 0.005$ Å for $x = 0$ to $a_F = 5.946 \pm 0.005$ Å for $x = 0.14$. Replacement in β-PbF_2 of Pb^{2+} by Ta^{5+} of clearly smaller size ought to lead to a smaller unit cell, but the simultaneous introduction of three additional F^- anions in interstitial sites is expected to lead to dilatation. These two opposing effects produce only a very weak increase of the unit cell.

Annealings of $Pb_{1-x}Ta_xF_{2+3x}$ at 400°C for 2 days yielded a low-temperature α phase for $0.14 < x < 0.15$ whose ideal composition should be Pb_6TaF_{17} $(x = 0.143)$. A high temperature X-ray diffraction study and DTA investigation of α-Pb_6TaF_{17} has shown that the allotropic transformation α-$Pb_6TaF_{17} \rightleftarrows \beta$-$Pb_6TaF_{17}$ is reversible and takes place at $t = 460 \pm 10$°C. The analysis of the X-ray pattern diffraction of α-Pb_6TaF_{17} shows a splitting of the fluorite-type reflections characteristic of an orthorhombic distortion (Table II). A subcell corresponds to the parameters $a_{\mathrm{subc.}} \simeq \sqrt{2}/2a_F$, $b_{\mathrm{subc.}} \simeq \sqrt{2}/2a_F$, $c_{\mathrm{subc.}} \simeq a_F$, where a_F is the parameter of the fluorite-type unit cell. The existence of extra lines reveals actually an orthorhombic superstructure whose parameters are $a_{\mathrm{ord.}} = a_{\mathrm{subc.}} \simeq \sqrt{2}/2a_F$, $b_{\mathrm{ord.}} = b_{\mathrm{subc.}} \simeq \sqrt{2}/2a_F$, $c_{\mathrm{ord.}} = 7c_{\mathrm{subc.}} \simeq 7a_F$. Crystallographic data obtained for α-$Pb_6TaF_{17\,\mathrm{ord.}}$ are $a = 4.284 \pm 0.002$ Å, $b = 4.110 \pm 0.002$ Å, $c = 41.15 \pm 0.05$ Å, with $Z = 2$ Pb_6TaF_{17} units.

TABLE II

X-RAY DIFFRACTION FOR ANNEALED Pb_6TaF_{17} (α FORM)

	Subcell		Superstructure			
hkl (cub.)	*hkl* (orth.)	$d_{cal.}$ (Å)	*hkl* (orth.)	$d_{cal.}$ (Å)	$d_{obs.}$ (Å)	I/I_0
			102	4.19	4.19	<5
			012	4.03	4.00	<5
			$01\underline{11}$	3.74	3.70	<5
			015	3.68		
111	101	3.462	107	3.462	3.470	100
	011	3.368	017	3.368	3.370	97
200	110	2.965	110	2.965	2.962	50
	002	2.939	$00\underline{14}$	2.939	2.938	40
			$10\underline{11}$	2.818	2.834	<5
			$00\underline{15}$	2.743	2.748	<5
			$11\underline{11}$	2.324	2.333	<5
	200	2.142	200	2.142	2.145	16
220	112	2.088	$11\underline{14}$	2.088	2.086	62
	020	2.055	020	2.055	2.057	16
			207	2.012	2.003	<5
			027	1.940	1.938	<5
			028	1.908	1.904	<5
			$20\underline{10}$	1.900		
	211	1.807	217	1.807	1.808	19
311	103	1.782	$10\underline{21}$	1.782	1.782	16
	013	1.769	$01\underline{21}$	1.769	1.769	34
	121	1.767	127	1.767	—	
222	202	1.731	$20\underline{14}$	1.731	1.733	12
	022	1.684	$02\underline{14}$	1.684	1.686	11
			$21\underline{12}$	1.662	1.664	<5
			$12\underline{11}$	1.660		
			$20\underline{16}$	1.646	1.644	<5
			$02\underline{15}$	1.645		

Pb_3TaF_{11} ($x = 0.25$) has a complex X-ray pattern whose main lines are listed in Table III.

Electrical Conductivity Investigation

The electrical conductivity has been measured on powder samples. The pellets used were sintered in large gold tubes sealed under argon at the same temperature as the powder samples. The compactness of the pellets was about 90%. Vacuum-evaporated gold has been used as electrodes. The bulk resistance has been measured by the complex impedance method using a "Solartron 1170" frequency response analyzer (*12*). The frequency range was 10^{-2}–10^4 Hz; measurements were carried out for several temperature cycles between 20 and 160°C.

Figure 1 shows the temperature dependence of the conductivity for several compositions of the $Pb_{1-x}Ta_xF_{2+3x}$ ($0 \leq x \leq 0.14$) solid solution. In the temperature range under study σ can be represented as $\sigma = A/T \exp(-\Delta E/kT)$, where A is constant and ΔE the activation energy related to the diffusive motion of the carriers.

Figures 2 and 3 give, respectively, the isotherm of conductivity corresponding to $t = 60°C$ and the variation of the activation energy ΔE as a function of substitution rate for the $Pb_{1-x}Ta_xF_{2+3x}$ solid solution. We have included on those figures the curves relative to the previously studied $Pb_{1-x}In_xF_{2+x}$ (*5*) and $Pb_{1-x}Zr_xF_{2+2x}$ (*7, 13*) solid solutions for the sake of comparison.

Three regions can be detected for the concentration dependence of the transport properties of the $Pb_{1-x}Ta_xF_{2+3x}$ solid solution.

TABLE III

MAIN LINES OF THE X-RAY DIFFRACTION FOR Pb_3TaF_{11}

$d_{obs.}$	I/I_0
4.75	4
3.736	35
3.686	55
3.622	10
3.471	35
3.362	24
3.312	100
3.240	11
3.176	9
2.974	19
2.625	5
2.148	7
2.131	29
2.091	27
2.066	8
2.008	7
1.978	7
1.854	16
1.789	14
1.733	8
1.663	8

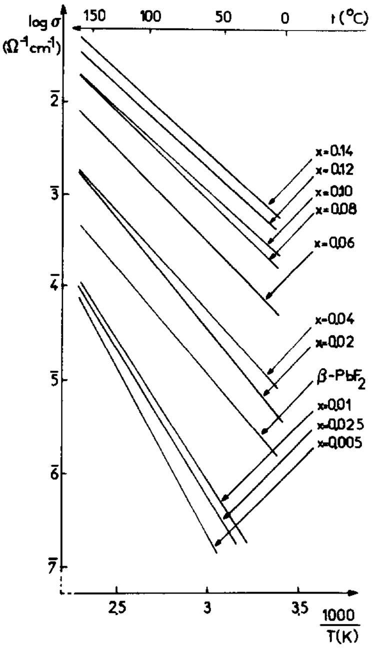

FIG. 1. Variation of log σ with reciprocal temperature for various compositions of the $Pb_{1-x}Ta_xF_{2+3x}$ solid solution.

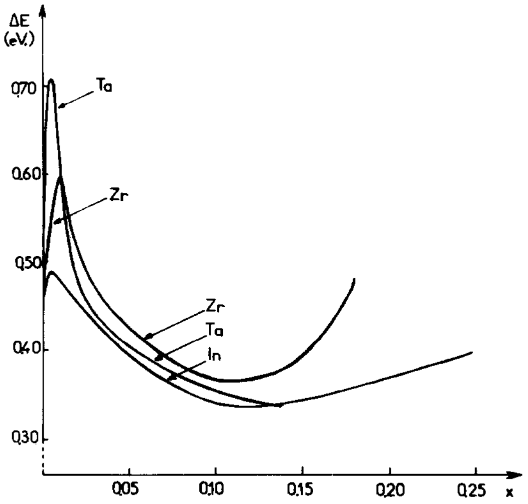

FIG. 3. Composition dependence of the activation energy for the $Pb_{1-x}In_xF_{2+x}$, $Pb_{1-x}Zr_xF_{2+2x}$, and $Pb_{1-x}Ta_xF_{2+3x}$ solid solutions.

A dilute concentration region ($x \lesssim 0.005$) where the conductivity decreases and the activation energy simultaneously increases.

An intermediate concentration region ($0.005 \lesssim x \lesssim 0.05$) where one observes a very large increase in conductivity associated with a large drop in activation energy.

A solid solution region with a higher tantalum concentration ($0.05 \lesssim x \lesssim 0.14$) where the enhancement of transport properties is weaker.

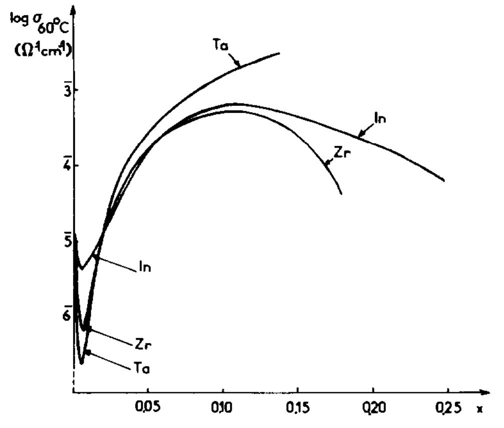

FIG. 2. Composition dependence of the conductivity at t = 60°C for the $Pb_{1-x}In_xF_{2+x}$, $Pb_{1-x}Zr_xF_{2+2x}$, and $Pb_{1-x}Ta_xF_{2+3x}$ solid solutions.

The first two regions are similar to those previously observed for $Pb_{1-x}In_xF_{2+x}$ and $Pb_{1-x}Zr_xF_{2+2x}$ (Figs. 2 and 3). The three solid solutions are characterized by the existence of a conductivity minimum associated with a maximum activation energy for a small value of the substitution parameter x_{min} ($0.005 \lesssim x_{min} \lesssim 0.01$). x_{min} seems independent of the nature of substitutional cation; by contrast the values of ΔE_{max} corresponding to x_{min} are quite different: ΔE_{max} = 0.71 eV for Ta^{5+}, 0.60 eV for Zr^{4+}, 0.49 eV for In^{3+}. For those three cations with similar sizes ΔE_{max} is a quasilinear function of the formal ionic charge. This result indicates that the increase of activation energy observed for the very small values of x could be due either to a tendency of the first substitutional cations introduced into β-PbF_2 to trap the F^- ions locally (*13*), or to residual traces of oxygen (*14*) producing isolated defect pairs which block the fluorine motion (*15*).

The composition dependence of the electrical properties of the three solid solutions for $x \gtrsim 0.05$ is quite different for $Pb_{1-x}Ta_xF_{2+3x}$ as compared to $Pb_{1-x}In_xF_{2+x}$ and $Pb_{1-x}Zr_xF_{2+2x}$. Indeed, a maximum of conductivity associated with a minimum of activation energy for the lead–indium and lead–zirconium solid solutions, respectively, at $x_{max} = 0.12$ and 0.10 has not been detected for the lead–tantalum solid solution. Quite likely the very small range of existence did not permit its detection.

In the composition range of the three solid solutions characterized by an increasing disorder, $x_{min} < x < x_{max}$ for $Pb_{1-x}In_xF_{2+x}$ and $Pb_{1-x}Zr_xF_{2+2x}$ and $x_{min} < x < 0.14$ for $Pb_{1-x}Ta_xF_{2+3x}$ the evolution of the electrical properties is similar. We suppose that the local defects are similar, due to the relatively small size difference between the substitutional cations, which accounts for the closeness of the electrical properties for a given value of x.

Neutron diffraction studies of the $Pb_{1-x}Bi_xF_{2+x}$ ($0 \leq x \leq 0.50$) and $Pb_{1-x}Th_xF_{2+2x}$ ($0 \leq x \leq 0.25$) solid solutions have shown that the intermediate compositions which have the best electrical performances are characterized by a maximum disorder (*9, 10*). For $x > x_{max}$ the conductivity decrease would result from the establishment of local order which should become progressively of the long range type for the compositions near the upper limit. Furthermore, these studies have shown that the boundary compositions which can be written $Pb_{0.50}Bi_{0.50}F_{I_{1.50}}F_{II}V_{F_{I_{0.50}}}$ and $Pb_{0.75}Th_{0.25}F_{I_{1.50}}F_{II_1}V_{F_{I_{0.50}}}$ (where F_I and F_{II} represent F^- ions in, respectively, normal and interstitial sites and V_{F_I} vacancies in normal sites) verify the following substitution mechanisms

$$Pb^{2+} + F_I^- = Bi^{3+} + 2\ F_{II}^- + V_{F_I}$$

$$Pb^{2+} + 2\ F_I^- = Th^{4+} + 4\ F_{II}^- + 2\ V_{F_I}$$

These mechanisms suppose that the replacement of one Pb^{2+} ion by one Bi^{3+} (or Th^{4+}) involves two (or four) F^- ions in interstitial sites with the production of one (or two) V_{F_I} vacancy(ies).

The adaptation of such models to $Pb_{1-x}Ta_xF_{2+3x}$ ($Pb^{2+} + 3\ F_I^- = Ta^{5+} + 6\ F_{II}^- + 3\ V_{F_I}$) would lead to the formula $Pb_{0.86}Ta_{0.14}F_{I_{1.58}}F_{II_{0.84}}V_{F_{I_{0.42}}}$ for the upper limit of the lead–tantalum solid solution. In such a formulation the number of interstitial fluorine atoms and vacancies would be close to those of the intermediate compositions, with the best performances within the lead–bismuth and lead–thorium solid solution ranges, $Pb_{0.75}Bi_{0.25}B_{I_{1.66}}F_{II_{0.59}}V_{F_{I_{0.34}}}$ and $Pb_{0.875}Th_{0.125}F_{I_{1.45}}F_{II_{0.80}}V_{F_{I_{0.55}}}$ (*9, 10*). A neutron diffraction study of $Pb_{1-x}Ta_xF_{2+3x}$, now in progress, will allow us to determine the distribution of fluorine atoms over nor-

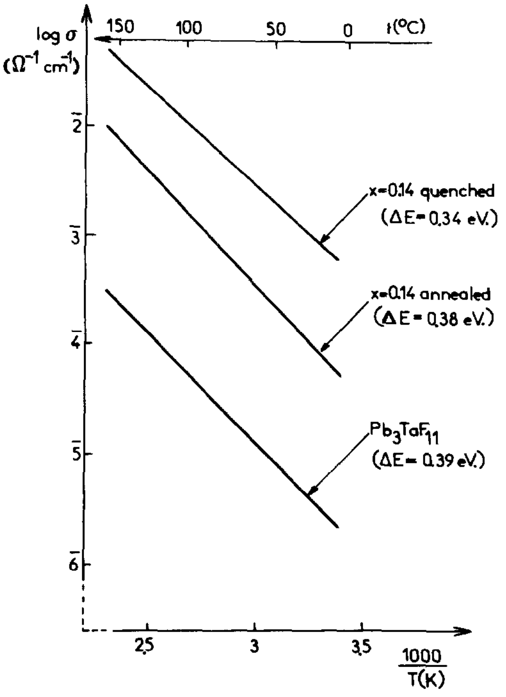

FIG. 4. Variation of log σ with reciprocal temperature for disordered and ordered $Pb_{0.86}Ta_{0.14}F_{2.42}$ varieties and Pb_3TaF_{11}.

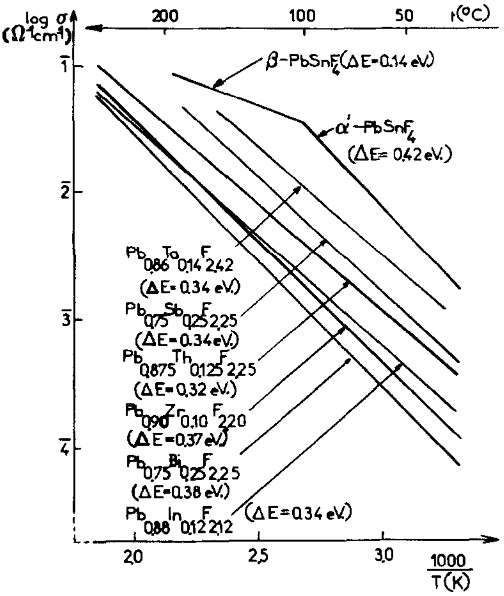

FIG. 5. Temperature dependence of the conductivity of some fast fluorine ion conductors.

mal and interstitial sites as a function of composition and to check this hypothesis.

The Ordered Phases

Figure 4 shows the temperature dependence of the conductivity for disordered $Pb_{0.86}Ta_{0.14}F_{2.42}$ prepared by quenching from 500°C and ordered $Pb_{0.86}Ta_{0.14}F_{2.42}$ obtained by a 2-day anneal at 400°C. As expected, the disordered phase exhibits better characteristics than the ordered one. A similar result had been obtained for disordered and ordered $Pb_{0.833}Zr_{0.167}F_{2.333}$ phases (*7*).

We have likewise plotted on Fig. 4 the temperature dependence of the conductivity for Pb_3TaF_{11}. As expected, the ordered phase is characterized by electrical performances clearly poorer than those of the $Pb_{1-x}Ta_xF_{2+3x}$ compositions corresponding to $x > 0.05$.

Figure 5 refers to the Arrhénius plots of conductivity of $Pb_{0.86}Ta_{0.14}F_{2.42}$ and some fast fluorine ion conductors. The electrical performance of $Pb_{0.86}Ta_{0.14}F_{2.42}$ place this material among the best of the F^- ionic conductors.

Acknowledgments

The authors express their sincere thanks for critical discussions with Dr. S. F. Matar, Lebanese University, Faculty of Sciences II, Mansourieh, Matn., P.O. Box 72, Lebanon.

References

1. J. M. REAU AND J. PORTIER, *in* "Solid Electrolytes, Fluorine Ion Conductors" (P. Hagenmuller and W. Van Gool, Eds.), Chap. 19, Academic Press, New York/London (1978).
2. P. HAGENMULLER, J. M., REAU, C. LUCAT, S. MATAR, AND G. VILLENEUVE, *Solid State Ionics*, **3/4,** 341 (1981).
3. J. M. REAU, S. B. TIAN, A. RHANDOUR, S. MATAR, AND P. HAGENMULLER, *Solid State Ionics*, in press.
4. C. LUCAT, A. RHANDOUR, J. M. REAU, J. PORTIER, AND P. HAGENMULLER, *J. Solid State Chem.* **29,** 373 (1979).
5. J. M. REAU, S. MATAR, S. KACIM, J. C. CHAMPARNAUD-MESJARD, AND B. FRIT, *Solid State Ionics* **7,** 165 (1982).
6. PH. DARBON, J. M. REAU, AND P. HAGENMULLER, *Mater. Res. Bull.* **16,** 273 (1981).
7. PH. DARBON, J. M. REAU, P. HAGENMULLER, C. DEPIERREFIXE, J. P. LAVAL, AND B. FRIT, *Mater. Res. Bull.* **16,** 389 (1981).
8. J. M. REAU, A. RHANDOUR, C. LUCAT, J. PORTIER, AND P. HAGENMULLER, *Mater. Res. Bull.* **13,** 827 (1978).
9. C. LUCAT, J. PORTIER, J. M. REAU, P. HAGENMULLER, AND J. L. SOUBEYROUX, *J. Solid State Chem.* **32,** 279 (1980).
10. J. L. SOUBEYROUX, J. M. REAU, S. MATAR, C. LUCAT, AND P. HAGENMULLER, *Solid State Ionics* **2,** 215 (1981).
11. R. D. SHANNON, *Acta Crystallogr. Sect. A* **32,** 751 (1976).
12. J. F. BAUERLE, *J. Phys. Chem.* **30,** 2657 (1969).
13. PH. DARBON, J. M. REAU, AND P. HAGENMULLER, *Solid State Ionics* **2,** 131 (1981).
14. J. L. SOUBEYROUX, S. F. MATAR, J. M. REAU, AND P. HAGENMULLER, *Solid State Ionics* **14,** 337 (1984).
15. C. R. A. CATLOW, *Solid State Ionics* **8,** 89 (1983).